Coral Reefs (2019) 38:395–403
https://doi.org/10.1007/s00338-019-01807-7

REPORT

Hiding in plain sight: invasive coral *Tubastraea tagusensis* (Scleractinia:Hexacorallia) in the Gulf of Mexico

Diego F. Figueroa[1] · Amelia McClure[2] · Nicole J. Figueroa[1] · David W. Hicks[1]

Received: 22 October 2018 / Accepted: 23 April 2019 / Published online: 7 May 2019

Abstract Our research presents the first record of *Tubastraea tagusensis* (Wells, Notes on Indo-Pacific scleractinian corals. Part 9. New corals from the Galápagos Islands, 1982) in the Gulf of Mexico. Specimens of *Tubastraea* were collected from various artificial reefs. Morphological analyses of these specimens show that there are three distinct lineages of *Tubastraea* that have remained cryptic due to similar morphology in the field: *Tubastraea coccinea* (Lesson, 1829), *T. tagusensis*, and a third clade containing a mix of characters of the former two. These results based on morphology are corroborated by phylogenetic and haplotype analyses using a partial sequence of the mitochondrial genes ATP8 and cytochrome oxidase I (mtCOI). The negative effects on natural habitats by invasive species of *Tubastraea* have been documented worldwide. Therefore, it is imperative to implement management policies that will help prevent the expansion of these species into natural habitats in the Gulf of Mexico. The essential first step is accurate identification to determine possible sources, vectors, and current expansion rates. We present a clear set of morphological characters and a genetic marker to help distinguish between these three cryptic lineages.

Keywords *Tubastraea tagusensis* · *Tubastraea coccinea* · Invasive coral · Gulf of Mexico · Phylogeny · Taxonomy

Topic Editor Morgan S. Pratchett

Electronic supplementary material The online version of this article (https://doi.org/10.1007/s00338-019-01807-7) contains supplementary material, which is available to authorized users.

✉ Diego F. Figueroa
diego.figueroa@utrgv.edu

[1] School of Earth, Environmental, and Marine Sciences, University of Texas Rio Grande Valley, One West University Boulevard, Brownsville, TX 78520, USA

[2] Department of Biology, University of Texas Rio Grande Valley, One West University Boulevard, Brownsville, TX 78520, USA

Introduction

One of the leading causes of biodiversity loss is the proliferation of invasive species. The threat and negative impacts of invasive species on local fauna have been documented in marine environments across the world (e.g., Cariton and Geller 1993; Secord 2003; Hollebone and Hay 2007; de Caralt and Cebrian 2013; Carlos-Júnior et al. 2015; Sammarco et al. 2015; Miranda et al. 2016). One of the most rapidly expanding invasive species in the Gulf of Mexico (GOM) and Western Atlantic is the scleractinian, orange cup coral, *Tubastraea coccinea* (e.g., Sammarco et al. 2004, 2010; Sampaio et al. 2012; Riul et al. 2013; Costa et al. 2014; da Silva et al. 2014; Precht et al. 2014; Sammarco et al. 2015; Batista et al. 2017; Capel et al. 2017). Present distribution of *T. coccinea* in the GOM suggests ships and oil and gas platforms as vectors for this invasive species (Fenner 2001; Sammarco et al. 2004; Sammarco 2007; Precht et al. 2014). In fact, artificial structures seem to be the preferred habitat for *T. coccinea*, which shows minimal presence on natural reefs in the GOM (Precht et al. 2014). A second invasive species of this genus, *Tubastraea micranthus* (Ehrenberg, 1834), was discovered in 2006 in the northern GOM (Sammarco et al. 2010). It is not as widespread as *T. coccninea*, but there are indications that it is expanding at a considerable rate in the northern GOM (Sammarco et al. 2014). The expanding populations of these two invasive species are of great

concern because of their potential for spreading from predominantly artificial habitats to natural reefs and banks.

Tubastraea species have successfully spread around the world, resulting in negative impacts to the environment and economy of the invaded region (Creed et al. 2017). Determining the most appropriate course of action to manage such invasions requires that we understand three key points: (1) Where did the invasive species originate? (2) How were they transported?, and (3) How are they spreading within the invaded region? These questions can be answered by looking at the geographical and temporal patterns of when an invasive species was first reported at a particular site and by studying genetic connectivity and phylogeography of the invasive species (i.e., Creed et al. 2017). These methods rely on accurate taxonomic identification of specimens. The misidentification of specimens could lead to erroneous conclusions and implementation of management policies that are ineffective and result in further damage to the environment and economy of the invaded region. In this research, we present evidence that *Tubastraea tagusensis* is a thriving invasive of the Gulf of Mexico. We show clear morphological differences between *T. tagusensis* and *T. coccinea* collected in the GOM, corroborated by genetic analyses of the mitochondrial gene cytochrome oxidase I (mtCOI).

Methods

Specimen collection

Specimens of *Tubastraea* spp. were collected by UTRGV divers at depths from 20 to 40 m. A total of 33 specimens were collected from artificial reefs (Fig. 1, Supplementary Table 1). Most came from the High Island oil field (28 specimens), the rest from Galveston-A-125 reef (2 specimens), East Breaks-110 Reef (2 specimens), and Texas Clipper (1 specimen). All specimens were preserved in ethanol in the field and subsequently stored in a − 20 freezer.

Morphological methods

Understanding the morphology of the coral skeleton is a key component in positive taxon identification. While there are many structures to consider, the septo-costa was the main structure used for morphological analysis for specimens of *Tubastraea* from the GOM. Within each corallite structure, or coral skeleton, there are thin, vertical rounded surfaces extending down to the center (columella) in radial cycles of these septo-costae that are distinct to each species (AIMS 2013). In some coral species, the septo-costae can be divided into two separate sections of the corallite by the outer wall or theca, where the septa are inside and the costae are outside (AIMS 2013). The septa are arranged in cycles of six that continue to multiple by a factor of six the further into each individual cycle all the way around the inner corallite and vary in length as well as thickness. For example, the first septal cycle is the most prominent and contains six septa, while the second cycle found in the middle of the first cycle is also composed of six septa. From here, we continue into the third septal cycle (S3) found in between septa one (S1) and septa two (S2) with 12 smaller septa making up the third cycle. The pattern continues with a fourth cycle found between S1 and S3 as well as S2 and S3 making a total of 24 septa and so on while getting smaller and smaller the further in (AIMS 2013). Different coral families vary in septo-costae morphology, but typically demonstrate two types of patterns, pourtales plan and Porites (AIMS 2013). *T. coccinea* and *T. tagusensis* belong to the family Dendrophylliidae which demonstrate a pourtales plan that is more primitive, where the fourth septal cycle curves in front of the third cycle and fuses with the next extending fourth septa (AIMS 2013). This fusion is a definitive attribute of the pourtales plan. Porites septa cycles have mostly straight septa descending to the columella without any fusion or fourth cycle extending past the third (AIMS 2013). Other defining features to distinguish morphological differences between *T. coccinea* and *T. tagusensis* include corallite diameter, columella diameter, and fossa length. The fossa is the space between the columella and the top of the corallite; in other words, it is the hollow area inside each coral skeleton down to the columella (de Paula and Creed 2004). The accurate identification of invasive species is critical for understanding their ecology and for the implementation of successful management policies. Therefore, in this study we list a set of clear morphological characteristics to help distinguish species of *Tubastraea* in the GOM.

The morphological analyses are largely based on the work of de Paula and Creed (2004) who reviewed the descriptions and revisions of *Tubastraea* species by Cairns (1991, 1994) and Wells (1982). Their detailed morphological analyses highlight the key differences between *T. coccinea* and *T. tagusensis* from specimens collected in Brazil, providing a list of characters that help distinguish these two species. Based on their work, the following characters were included in our morphological analyses: calicular diameter, columella diameter, corallite length, and fossa length.

Samples were prepared for morphological analyses by placing each specimen in a container filled with common household bleach (NaOCl). Submersing each sample in bleach allowed for the removal of all soft tissues, leaving only the coral skeleton. All samples were left in bleach until no tissue remained. Bleaching times ranged from a

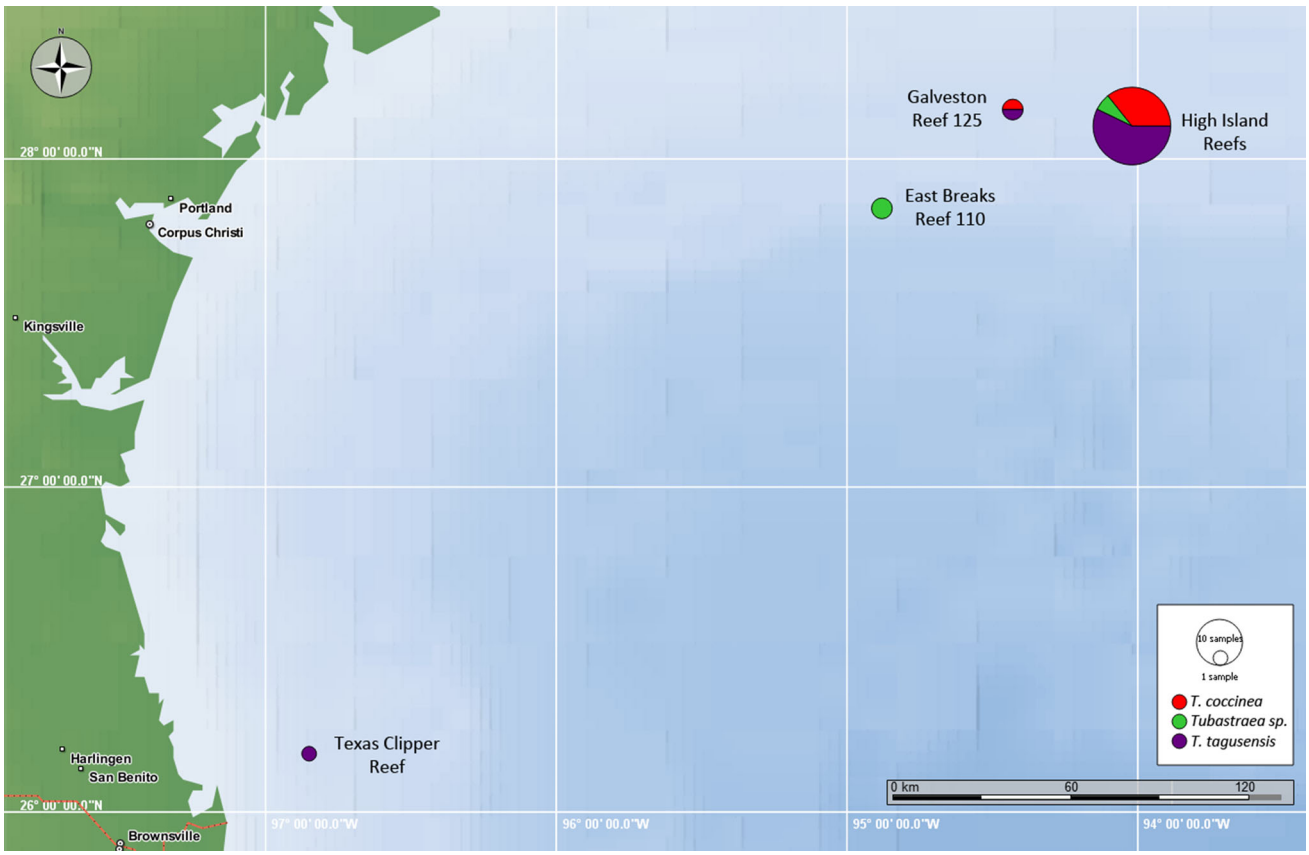

Fig. 1 Circles show the sampling locations of *Tubastraea* specimens in the GOM. Circle size corresponds to the number of specimens collected. Colors correspond to the three lineages: *Tubastraea coccinea* in red; *Tubastraea tagusensis* in purple; and an unidentified *Tubastraea sp.* in green. These lineages are defined based on morphological characters and partial sequences of mitochondrial genes ATP8 and COX1. Figure prepared with PopArt v 1.7.2

couple of days to a full week. Once the corallite structure was all that remained, bleach was emptied from each container and samples were rinsed with deionized water, then left to dry for 24–48 h. Measurements were taken from individual polyps in each specimen.

Molecular methods

A small tissue sample was taken from an individual polyp from each preserved specimen and rehydrated in molecular-grade water for at least 30 min. Genomic DNA was extracted by placing the tissue in a 2-ml tube with 100 µl of Bio-Rad's Instagene Matrix. The specimens were then placed in a thermomixer and incubated at 56 °C overnight. After incubation, samples were heated to 100 °C for 8 min. Samples were then centrifuged for 1 min at 10,000*g*. The supernatant containing the DNA was removed with a pipette and placed in a new 2-ml tube and then stored in a − 20 °C freezer. Quantification of extracted DNA was carried out using Thermofisher Scientific's Qubit fluorometer—set to OD_{260}. Samples containing at least 0.1 ng μl^{-1} of DNA were subjected to polymerase chain reaction (PCR) to amplify a 980 bp mitochondrial region that includes the end of ATP8 and the first half of cytochrome oxidase I. The primers used were designed by Lin et al. (2011), Cs-F16 (5′-TTAGGTTAAAGTAGACC GTTAGCC) and Cs-R16 (5′-ATCCGTTAAAAGCAT GGTTATGG). Polymerase chain reaction was carried out in a 25 µl reaction: 12.05 µl PCR water, 2.5 µl Invitrogen's 10X PCR Rxn Buffer, 1.25 µl Invitrogen's 50 mM MgCl–2, 2.0 µl of 10 mM dNTP, 1.0 µl of 10 mM forward primer (Cs-F16), 1.0 µl of 10 mM reverse primer (Cs-R16), 0.2 µl Thermo Fisher's Invitrogen Platinum TAQ DNA Polymerase, and 5.0 µl DNA. The following thermocycler conditions were employed: 95 °C for 3 min, followed by 30 cycles of 94 °C for 30 s, 48 °C for 45 s, 72 °C for 1.5 min, followed by 72 °C for 10 min, and then cooled at 4 °C ∞.

PCR products were visualized by agarose-gel electrophoresis followed by staining with 0.2 µg ml^{-1} ethidium bromide. Life Technology's Invitrogen 1 KB Plus DNA ladder (1.0 µg μl^{-1}) was used with each gel to determine whether a DNA band of the expected size ($\sim$ 980 bp) was amplified and to verify that other bands

were not present. The PCR products with a single band of ~ 980 bp were purified using Sigma Aldrich's GenElute PCR cleanup kit. Purified PCR products were sequenced by Sanger sequencing technique by Eurofins MWG Operon LLC with the forward and reverse primers.

Bioinformatics

For each specimen, the sequences for the forward and reverse strands were assembled with the software CLC Workbench 7.9.1 (CLC Bio, Aarhus, Denmark) using default settings. Chromatograms were visually inspected for conflicts between the two strands, and conflicts were resolved manually. Base quality scores were visually examined for quality control, and a consensus sequence was generated from the assembly. These sequences were used for all phylogenetic analyses along with two sequences extracted from full mitochondrial genomes deposited in GenBank (National Center for Biotechnology Information): one from *T. coccinea* (KX024566) and the other from *T. tagusensis* (KX024567). Both sequences are from a study by Capel et al. (2017) from specimens collected in Sao Sebastiao channel, Brazil.

Sequences were aligned with MUSCLE v3.8 (Edgar 2004) using default parameters (Edgar 2004) as implemented by Qiagen's CLC Main workbench and visually inspected for consistency. This alignment was used in phylogenetic analyses using maximum likelihood (ML) and Bayesian methods. The model of evolution and partitioning scheme was selected using PartitionFinder v1.1.1 (Lanfear et al. 2014) using linked branches and the AICc criterion. Blocks were defined by the two genes (ATP8 and COI) and codon position and the spacer (between ATP8 and COI). The ML analyses were performed using RAxML v8.0.0 (Stamatakis 2017) with 1000 bootstraps. For the ML analyses, PartitionFinder selected GTR + G for 3 partitions: 1) ATP8_pos2, Spacer, ATP8_pos3, ATP8_pos1; 2) COX1_pos1, COX1_pos3; and 3) COX1_pos2.

Mr. Bayes 3.1 (Ronquist and Huelsenbeck 2003) was used for the Bayesian analyses. For these analyses, PartitionFinder selected the following models and partitioning scheme: 1) F81 for ATP8_pos3, ATP8_pos1, Spacer; 2) F81 for COX1_pos2, ATP8_pos2; 3) HKY for COX1_pos1; and 4) HKY + G for COX1_pos3. Four chains were carried out for 1,100,000 generations, sampling every 200th generation. After inspecting the trace files generated by the Bayesian Markov Chain Monte Carlo (MCMC) runs, the initial 100,000 of sampled generations were omitted prior to building the consensus tree. Both phylogenies were rooted with *Dendrophyllia cribrosa* (JQ290080).

All the sequences recovered from our specimens were used for haplotype analyses. Haplotypes were defined by the software dnaSP v5 (Librado and Rozas 2009) which generated a haplotype list with gaps and missing sites considered and invariable sites included. This list was then used in a haplotype network analysis performed with PopArt v 1.7.2 (Leigh and Bryant 2015) using a median-joining network (with an epsilon of zero), which infers ancestral nodes by iteratively adding median sequence vectors (Leigh and Bryant 2015). By using inferred ancestors, the PopArt software deduces relationships between haplotypes and provides a straightforward, visual representation of those relationships. The size of the nodes in the haplotype network is weighted by the frequency of individuals in each haplotype.

An additional phylogenetic analysis was performed using all available *Tubastraea* sequences of mtCOI in GenBank (24 sequences, supplementary Table 2) and the haplotype sequences from this study. The same phylogenetic methods as described above were used for this analysis.

Results

Morphology

The samples analyzed exhibited three distinct morphologies (Fig. 2 and Table 1). Samples A1-9, B8, and B13 have a typical morphology for *T. coccinea*. Samples B1-7, B9-12, B16-17, and B21-24 exhibit morphology typical of *T. tagusensis*. The third group, which we will refer to as *Tubastraea* clade 2B (based on phylogenetic analyses), demonstrated a combination of characters from *T. coccinea* and *T. tagusensis*. *Tubastraea coccinea* demonstrates a typical pourtales plan with four septal cycles and clear fusion found on the fourth septa (de Paula and Creed, 2004). Figure 2a illustrates where each septa can be found in a radial pattern. The fourth cycle can be very thin and fragile; therefore, not all cycles are represented; however, S4 is normally present in this species. Figure 2b demonstrates a distinctive *T. coccinea* curved septa cycle at S4 within the corallite indicating plentiful fusion as well as a large columella in the middle. The diameter of columella found in the specimens used for this study ranged from 0–11 mm, with an average of 2.3 mm. Corallite diameter for this species demonstrated an average of 7.47 mm, ranging from 4.5 to 18.75 mm. Fossa length is shallower in comparison with *T. tagusensis*, demonstrating a range of 1–9 mm, with an average of 3.8 mm. *Tubastraea coccinea* total corallite length from the base to the top is usually rather short with an average length of 6 mm; however, they ranged from 1 to 17 mm.

Although *T. tagusensis* does not exhibit any fusion between septa, it is still indicative of a pourtales plan due to

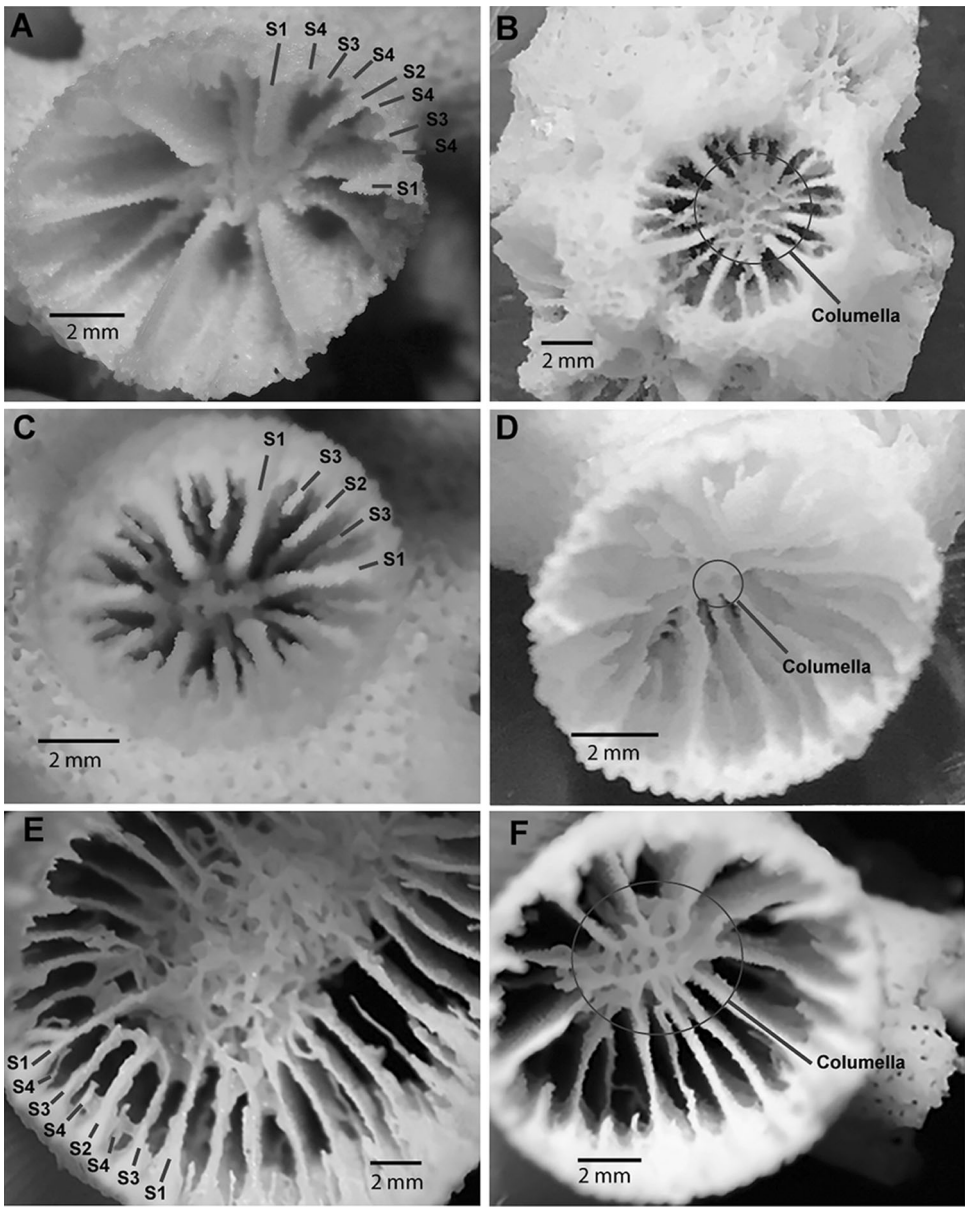

Fig. 2 Septal cycle, septal fusion, and columella of: *Tubastraea coccinea* (**a** and **b**) four septa cycles, S4 fused, columella large; *Tubastraea tagusensis* (**c** and **d**) three, sometimes four septa cycles, no fusion, columella small or absent; and *Tubastraea sp.* (**e** and **f**) four septa cycles, S3 and/or S4 fused, columella large. Photographed by Amelia McClure

the curvature of its septal cycles as well as an occasional fourth septa, while three cycles are most often found (de Paula and Creed, 2004) as seen in Fig. 2c, d). The columella diameter is very small, rarely more than two millimeters and sometimes barely present at all in some organisms (de Paula and Creed 2004). The observed columella diameter of the samples used here ranged from 0 to 3.75 mm, with an average of 1.43 mm. Corallite diameter is normally smaller than that of *T. coccinea*, our specimens of *T. tagusensis* had an average diameter of 6.5 mm, almost 1 mm less than that of specimens of *T. coccinea,* with a range of 3–12 mm. Fossa is much deeper in this species, which consequently means the overall length of the whole corallite is longer. Fossa length for *T. tagusensis* was as much as 15 mm, with an average of 5.2 mm. Corallite length from the base had a maximum of 29 mm, with an average of 8.8 mm.

The new clade of *Tubastraea* exhibits many characteristics of both *T. tagusensis* and *T. coccinea*, especially in corallite morphology. Figure 2e, f) shows the septal pattern, septal fusion, and columella. They appear to follow the same pourlates plan indicative of the Dendrophylliidae family; however, the septo-costae pattern seems less clear. This species is large and extends further than either *T. tagusensis* or *T. coccinea* from the base to the top of the corallite with a maximum length of 33.5 mm and an average of 27 mm. The columella diameter is also very large varying from 3.5 to 10 mm, with an average of 5.83 mm. Corallite diameter measured as much as

Table 1 Quantitative and qualitative characteristics of *Tubastraea* specimens

	T. coccinea	*T. tagusensis*	Tubastraea (clade 2B)
Sample size (polyps)	95	71	3
Corallite diameter			
Range (mm)	4.5–18.8	3.0–12.0	10.0–18.3
Average (mm)	7.5 ± 0.4	6.5 ± 0.4	13.0 ± 4.2
Columella diameter			
Range (mm)	0–11.0	0–3.8	3.5–10.0
Average (mm)	2.1 ± 0.3	1.4 ± 0.8	5.8 ± 3.3
Corallite length			
Range (mm)	1.0–17.0	1.0–29.0	23.5–33.5
Average (mm)	6.0 ± 0.7	8.8 ± 1.7	27.0 ± 5.2
Fossa length			
Range (mm)	1.0–9.0	1.0–15.0	11.0–14.5
Average (mm)	3.8 ± 0.4	5.2 ± 0.8	12.7 ± 1.6
Corallite projection			
Range (mm)	0.75–15	1–15.5	12.5–18.8
Average (mm)	5.03 ± 0.7	5.6 ± 0.97	15.6 ± 4.3
Septa cycle	S1, S2, S3, S4	S1, S2, S3 (S4 sometimes present)	S1, S2, S3, S4
Septa fusion	S4 fused	No fusion	S3 and/or S4 Fused

18.25 mm and a very deep fossa length with an average of 12.67 mm.

Phylogeny

Only 22 specimens yielded DNA and PCR product of high quality. These 22 sequences along with three sequences from Genbank, *T. coccinea* (KX024566), *T. tagusensis* (KX024567), and the outgroup *Dendrophyllia cribrosa* (JQ290080) were used in a final alignment of 859 base pairs. The phylogenetic reconstruction using ML and Bayesian methods shows similar topology (Fig. 3). Two major clades were recovered. The first diverging clade (clade 1) included all specimens exhibiting the basic *T. tagusensis* morphology along with *T. tagusensins* sequence KX024567 with strong support from both ML (97 bootstrap) and Bayesian (100 posterior probability) methods. The second clade (clade 2) has strong support from the Bayesian reconstruction (92 posterior probability) but weaker support from the ML reconstruction (66 bootstrap). This second clade is further divided into two sub-clades, one (clade 2A) containing all specimens exhibiting the typical *T. coccinea* morphology along with *T. coccinea* sequence KX024566. This sub-clade has strong support from the ML analyses (71 bootstrap). The Bayesian analyses also recovered this clade, but its support was not statistically significant (< 50 posterior probability). The second sub-clade (clade 2B) contains all specimens exhibiting mixed morphological characteristics of both *T. coccinea* and *T. tagusensis*. This sub-clade has statistically significant support from the Bayesian methods (54 posterior probability). The ML method also recovered this clade but its support was not statistically significant (< 50 bootstrap).

The 22 sequences from our *Tubastraea* specimens generated six unique haplotypes (Fig. 3). The sequence for one representative from each haplotype was entered in GenBank (accession # MK077638-MK077643). Each major lineage had one dominant haplotype, and each had one specimen with a haplotype that span out from each dominant haplotype by a single mutation. The dominant haplotype for *Tubastraea* clade 2b is most closely related to *T.coccinea*, separated by a single mutation; while the dominant haplotype for *T. tagusensis* is separated by four mutations from that of *Tubastraea* clade 2b and by five mutations from that of *T. coccinea*. The results from the haplotype analyses are consistent with the phylogenetic analyses.

The six haplotypes generated were used for an additional phylogenetic analysis with 24 sequences of mtCOI available in GenBank from various *Tubastraea* species from around the world. The 24 sequences included specimens of *T. coccinea* (6), *T. tagusensis* (1), *T. micranthus* (4), *T. aurea* (7), and unidentified *Tubastrae sp.* (6). Most of these sequences were from a study by Arrigoni et al. (2014) who targeted a 750 bp region of mtCOI. Our sequences only overlapped 421 bp of this targeted region. So our analysis was based on a 421 bp alignment. Both the maximum likelihood and Bayesian phylogenetic reconstruction show similar topology (Supplementary Fig. 1). There were only two major clades supported with all other relationships remaining unresolved. One of the well-

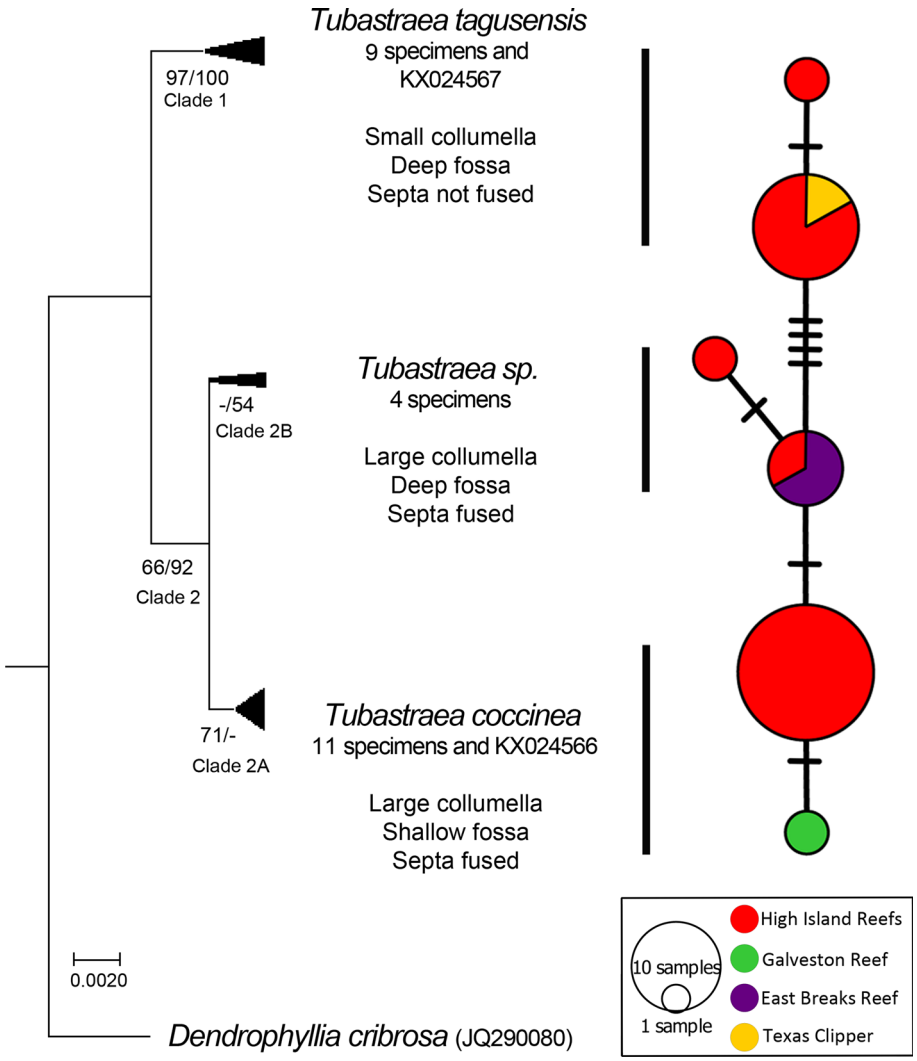

Fig. 3 Molecular analysis of *Tubastraea* based on partial sequence of mitochondrial genes ATP8 and COI. Left side shows phylogenetic reconstruction using maximum likelihood and Bayesian methods. Tree rooted with *Dendrophyllia cribrosa* (JQ290080). Branch labels correspond to bootstrap support and posterior probabilities. A dash (−) indicates support values < 0.50. Branches are collapsed, showing the three major clades of *Tubastraea*. Right side shows median-joining network analysis. The size of the node reflects the haplotype frequency. Notches on each branch represent the number of nucleotide changes between haplotypes. The color of each node represents the location where the specimen was collected

supported clades included our two haplotypes of *T. tagusensis*, the *T. tagusensis* sequence from Brazil, and two sequences of *T. micranthus*. The second well-supported clade contained our two haplotypes of *T. coccinea*, our two haplotypes of *Tubastrase sp.* (clade 2b), three sequences of *T. coccinea*, and seven sequences of *T. aurea*.

Discussion

Our morphological and genetic analyses show three distinct groups of *Tubastraea*. The first group corresponds to *Tubastraea coccinea*. These specimens match the morphological descriptions for *T. coccinea* (reviewed by de Paula and Creed 2004) with a large collumella, shallow fossa, and fused septa. This group is strongly supported by the phylogenetic and haplotype network analyses (Fig. 3). The second group belongs to *Tubastraea tagusensis*. The morphology of these specimens shows a small collumella, deep fossa, and independent septa, all distinguishing characteristics of *T. tagusensis* (reviewed by de Paula and Creed 2004). This group is also strongly supported by the phylogenetic and haplotype network analyses (Fig. 3). The third group of *Tubastraea* has mixed characteristics; similar to *T. coccinea*, it has a large collumella and fused septa; but similar to *T. tagusensis*, it has a deep fossa and longer corallite length. The characteristics that set this group apart from both *T. coccinea* and *T. tagusensis* are greater polyp diameter (about two times larger) and greater polyp length (about three times larger) than either species. The phylogenetic analyses recovered this group as an independent, but weakly supported clade. The phylogeny and haplotype network also shows that this clade is more closely related to *T. coccinea* than to *T. tagusensis*. Whether this group is a new species of *Tubastraea*, a subspecies of *T. coccinea*, or a hybrid of *T. coccinea* and *T. tagusensis* will require detailed morphological analyses of all *Tubastraea* species combined with a comprehensive phylogenetic analyses that in addition to mitochondrial genes also uses nuclear genes. Arrigoni et al. (2014) did such an

analysis for species of the family Dendrophylliidae, which include *Tubastraea*. Their analysis included four species of *Tubastraea* (*T. coccinea*, *T. aurea*, *T diaphana*, and *T. micranthus*) along with three additional unidentified species of this genus. They targeted two mitochondrial (COI and IGR) and one nuclear (ITS1) marker. Their results show that phylogenetic reconstructions based on the mitochondrial markers leave most relationships unresolved, while the nuclear marker provides a more robust topology. When all three are combined, their phylogeny shows that all *Tubastraea* species are monophyletic. We show similar results of a largely unresolved phylogeny when using the reduced, overlapping fragment, of COI. A future analysis that targets all three markers (COI, IGR, and ITS1) would be useful in determining the phylogenetic position of this new clade (clade 2b) of *Tubastraea* from the GOM. Accurate taxonomy is an essential first step to understanding the invasion history of Tubastraea species in the GOM.

Tubastraea coccinea is a coral native to the Indo-Pacific, and it is believed to have been introduced by ships to the Western Atlantic Ocean in the early 1900s, with the first documented specimen identified in 1951 (Cairns 2000). The expansion of this invasive in the GOM across oil platforms has been extensively documented (e.g., Sammarco et al. 2004, 2012; Sammarco 2013, 2015; Precht et al. 2014). *Tubastraea tagusensis* was first described from the Galapagos Islands in the eastern Pacific (Wells 1982). It is now considered an invasive species in the Southwestern Atlantic, first described in coastal waters in Brazil by de Paula and Creed (2004). The expansion of *T. tagusensis* in Brazilian waters and the negative impacts associated with this invasive species has been the subject of much research (e.g., de Paula and Creed 2004; da Silva et al. 2014; Carlos-Júnior et al. 2015; Mantelatto et al. 2015; Miranda et al. 2016; Capel et al. 2017; Luz and Kitahara 2017). In Brazil, *T. tagusensis* has a larger range and it is more abundant than its congener *T. coccinea* (da Silva et al. 2014), which was first recorded in Brazilian waters in the late 1990s (Castro and Pires 2001). We show a similar pattern of dominance by *T. tagusensis* in the GOM. Even though our sampling was limited to thirty-three specimens, these were collected at random with the majority (55%) belonging to *T. tagusensis*. *Tubastraea* species have been expanding their range in Brazil for over a decade where they have displaced native fauna in natural reefs (da Silva et al. 2014). The GOM species of *Tubastraea* are almost exclusively found on artificial structures, but they have started to expand into natural habitats. *Tubastraea coccinea* was first discovered on a natural bank in the GOM in 2002 at the East Flower Garden Bank (Sammarco et al. 2004). In 2004, numerous colonies were found on Geyer Bank, doubling in numbers by 2007 (Precht et al. 2014). By 2012, *T. coccinea* had not only increased by an order of magnitude on Geyer Bank, but colonies were also found in West Flower Garden Bank and Stetson Bank Precht et al. 2014). These natural banks are in close proximity to the artificial reefs that we sampled in the High Island oil field. Accurate identification of *Tubastraea* species in the GOM is essential for implementing management policies that will help prevent their expansion into natural habitats. Understanding the spread of invasive species requires the determination of possible sources, vectors, and current expansion rates. All of which are impossible to asses when invasive species are misidentified.

Due to the cryptic nature of *T. tagusensis* in the GOM, it is not clear whether previous studies of *T. coccinea* also included misidentified specimens of *T. tagusensis*. It would be worthwhile to investigate past collections to determine whether misidentifications have occurred. This would aid in establishing the likely date and place of introduction of *T. tagusensis* in the GOM. If previous collections include specimens that were kept frozen or preserved in ethanol, then genetics could also be used to aid in this endeavor. If *T. tagusensis* has not been reported before from the GOM because it is truly a new arrival, then our study suggests that it is expanding at a rapid rate and outcompeting *T. coccinea*, making it a greater threat to native species in the GOM.

Acknowledgements We would like to thank the Texas Parks and Wildlife Department—Artificial Reef Program (TPWD-ARP) for allowing UTRGV divers (Heather Otte, Chelsea Pavliska, and Linda Jordan) to join their annual biological monitoring trips to the Galveston, High Island, and East Breaks lease block areas in the Gulf of Mexico for specimen collection. Specimen collections of the south Texas coast were supported by TPWD-ARP (Grant No. 475342, 2016–2018) to David Hicks. Research reported in this publication was supported in part by startup funds from the University of Texas Rio Grande Valley to Diego Figueroa, by the Gulf Research Program of the National Academies of Sciences, Engineering, and Medicine under the Grant Agreement number 2000007266 to Diego Figueroa, and by Publication supported in part by an Institutional Grant (NA14OAR4170102 to Diego Figueroa and David Hicks) to the Texas Sea Grant College Program from the National Sea Grant Office, National Oceanic and Atmospheric Administration, U.S. Department of Commerce. The content is solely the responsibility of the authors and does not necessarily represent the official views of the Gulf Research Program or the National Academies of Sciences, Engineering, and Medicine.

Compliance with ethical standards

Conflict of interest On behalf of all authors, the corresponding authors state that there is no conflict of interest.

References

Arrigoni R, Kitano YF, Stolarski J, Hoeksema BW, Fukami H, Stefani F, Galli P, Montano S, Castoldi E, Benzoni F (2014) A phylogeny reconstruction of the Den-drophylliidae (Cnidaria, Scleractinia)

based on molecular and micromorphological criteria, and its ecological implications. Zoologica Scripta 43:661–688
Batista D, Gonçalves JEA, Messano HF, Altvater L, Candella R, Elias LMC, Messano D, Resende LV, Apolinário M, Coutinho R (2017) Distribution of the invasive orange cup coral Tubastraea coccinea Lesson, 1829 in an upwelling area in the South Atlantic Ocean 15 years after its first record. Aquat Invasions 12:23–32
Cairns SD (1991) A revision of the ahermatypic Scleractinia of the Galápagos and Cocos Island. Smithsonian Istitution Press, Washington
Cairns SD (1994) Scleractinia of the temperate North Pacific. Smithsonian Istitution Press, Washington
Cairns SD (2000) A revision of the shallow water azooxanthellate scleractinia of the Western Atlantic, vol 75. Studies of the Natural History of the Caribbean Region, pp 1–231
Capel KCC, Toonen RJ, Rachid CT, Creed JC, Kitahara MV, Forsman Z, Zilberberg C (2017) Clone wars: asexual reproduction dominates in the invasive range of Tubastraea spp. (Anthozoa: Scleractinia) in the South-Atlantic Ocean. PeerJ 5:e3873
Cariton JT, Geller JB (1993) Ecological roulette: the global transport of nonindigenous marine organisms. Science 261:78–82
Carlos-Júnior LA, Neves DM, Barbosa NPU, Moulton TP, Creed JC (2015) Occurrence of an invasive coral in the southwest Atlantic and comparison with a congener suggest potential niche expansion. Ecol Evol 5:2162–2171
Castro CB, Pires DO (2001) Brazilian coral reefs: what we already know and what is still missing. Bull Mar Sci 69:357–371
Costa TJ, Pinheiro HT, Teixeira JB, Mazzei EF, Bueno L, Hora MS, Joyeux J-C, Carvalho-Filho A, Amado-Filho G, Sampaio CL (2014) Expansion of an invasive coral species over Abrolhos Bank, Southwestern Atlantic. Mar Pollut Bull 85:252–253
Creed JC, Fenner D, Sammarco P, Cairns S, Capel K, Junqueira AO, Cruz I, Miranda RJ, Carlos-Junior L, Mantelatto MC (2017) The invasion of the azooxanthellate coral Tubastraea (Scleractinia: Dendrophylliidae) throughout the world: history, pathways and vectors. Biol Invasions 19:283–305
da Silva AG, de Paula AF, Fleury BG, Creed JC (2014) Eleven years of range expansion of two invasive corals (*Tubastraea coccinea* and *Tubastraea tagusensis*) through the southwest Atlantic (Brazil). Estuar Coast Shelf Sci 141:9–16
de Caralt S, Cebrian E (2013) Impact of an invasive alga (Womersleyella setacea) on sponge assemblages: compromising the viability of future populations. Biol Invasions 15:1591–1600
de Paula AF, Creed JC (2004) Two species of the coral Tubastraea (Cnidaria, Scleractinia) in Brazil: a case of accidental introduction. Bull Mar Sci 74:175–183
Edgar RC (2004) MUSCLE: multiple sequence alignment with high accuracy and high throughput. Nucleic Acids Res 32:1792–1797
Fenner D (2001) Biogeography of three Caribbean corals (Scleractinia) and the invasion of Tubastraea coccinea into the Gulf of Mexico. Bull Mar Sci 69:1175–1189
Hollebone AL, Hay ME (2007) Propagule pressure of an invasive crab overwhelms native biotic resistance. Mar Ecol Prog Ser 342:191–196
Lanfear R, Calcott B, Kainer D, Mayer C, Stamatakis A (2014) Selecting optimal partitioning schemes for phylogenomic datasets. BMC Evol Biol 14:82
Leigh JW, Bryant D (2015) popart: full-feature software for haplotype network construction. Methods Ecol Evol 6:1110–1116
Librado P, Rozas J (2009) DnaSP v5: a software for comprehensive analysis of DNA polymorphism data. Bioinformatics 25:1451–1452
Lin M-F, Luzon KS, Licuanan WY, Ablan-Lagman MC, Chen CA (2011) Seventy-four universal primers for characterizing the complete mitochondrial genomes of scleractinian corals (Cnidaria; Anthozoa). Zool Stud 50:513–524
Luz B, Kitahara M (2017) Could the invasive scleractinians Tubastraea coccinea and T. tagusensis replace the dominant zoantharian Palythoa caribaeorum in the Brazilian subtidal? Coral Reefs 36:875
Mantelatto MC, Pires LM, de Oliveira GJG, Creed JC (2015) A test of the efficacy of wrapping to manage the invasive corals Tubastraea tagusensis and T. coccinea. Management 6:367–374
Miranda RJ, Costa Y, Lorders FL, José de Anchieta CC, Barros F (2016) New records of the alien cup-corals (Tubastraea spp.) within estuarine and reef systems in Todos os Santos Bay, Southwestern Atlantic. Mar Biodivers Rec 9:35
Precht WF, Hickerson EL, Schmahl GP, Aronson RB (2014) The invasive coral Tubastraea coccinea (Lesson, 1829): implications for natural habitats in the Gulf of Mexico and the Florida Keys. Gulf Mexico Sci 32:5
Riul P, Targino CH, Júnior LA, Creed JC, Horta PA, Costa GC (2013) Invasive potential of the coral Tubastraea coccinea in the southwest Atlantic. Mar Ecol Prog Ser 480:73–81
Ronquist F, Huelsenbeck JP (2003) MrBayes 3: Bayesian phylogenetic inference under mixed models. Bioinformatics 19:1572–1574
Sammarco P (2007) Invasive species on oil and gas platforms in the northern Gulf of Mexico: Island--hopping and biogeographic expansion. In: 2007 Proceedings and final report of the Gulf of Mexico and Caribbean marine invasive species workshop held at Harte research institute for Gulf of Mexico studies, Texas A&M University--Corpus Christi, Corpus Christi, TX, Feb
Sammarco PW (2013) Corals on oil and gas platforms near the Flower Garden Banks: population characteristics, recruitment, and genetic affinity. US Dept of the Interior, Bureau of Ocean Energy Management, Gulf of Mexico OCS Region, New Orleans, LA OCS Study BOEM 216:106
Sammarco PW, Atchison AD, Boland GS (2004) Expansion of coral communities within the Northern Gulf of Mexico via offshore oil and gas platforms. Mar Ecol Prog Ser 280:129–143
Sammarco PW, Porter SA, Cairns SD (2010) New invasive coral species for the Atlantic Ocean: Tubastraea micranthus (Cairns and Zibrowius 1997) (Colenterata, Anthozoa, Scleractinia): a potential major threat? Aquat Invas 5:131–140
Sammarco PW, Brazeau DA, Sinclair J (2012) Genetic connectivity in scleractinian corals across the northern Gulf of Mexico: oil/gas platforms, and relationship to the Flower Garden Banks. PloS ONE 7:e30144
Sammarco PW, Porter SA, Sinclair J, Genazzio M (2014) Population expansion of a new invasive coral species, Tubastraea micranthus, in the northern Gulf of Mexico. Mar Ecol Prog Ser 495:161–173
Sammarco PW, Porter SA, Genazzio M, Sinclair J (2015) Success in competition for space in two invasive coral species in the western Atlantic-Tubastraea micranthus and *T. coccinea*. PloS ONE 10:e0144581
Sampaio CL, Miranda RJ, Maia-Nogueira R, José de Anchieta C (2012) New occurrences of the nonindigenous orange cup corals *Tubastraea coccinea* and *T. tagusensis* (Scleractinia: Dendrophylliidae) in Southwestern Atlantic. Check List 8:528–530
Secord D (2003) Biological control of marine invasive species: cautionary tales and land-based lessons marine bioinvasions: patterns, processes and perspectives. Springer, New York, pp 117–131
Stamatakis A (2017) RAxML Version 8: a tool for phylogenetic analysis and post-analysis of large phylogenies. Bioinformatics 30:1312–1313
Wells JW (1982) Notes on Indo-Pacific scleractinian corals. Part 9. New corals from the Galápagos Islands. Pac Sci 36:211–219